Polymer(Korea), Vol. 41, No. 4, pp. 694-701 (2017)
https://doi.org/10.7317/pk.2017.41.4.694

ISSN 0379-153X(Print)
ISSN 2234-8077(Online)

리그노술폰산을 함유한 폴리피롤 복합체의 전기전도도

M. Jeevan Kumar Reddy · 신보경 · 허도성†
인제대학교 화학 및 나노융합공학과
(2017년 1월 29일 접수, 2017년 3월 8일 수정, 2017년 3월 31일 채택)

Conductivity of Polypyrrole Composite Films Containing Lignosulfonic Acid

M. Jeevan Kumar Reddy, Bo Kyoung Shin, and Do Sung Huh†
Department of Chemistry and Nano Science and Engineering, Center for Nanomanufacturing, Inje University, Gimhae, Kyungnam 50834, Korea
(Received January 29, 2017; Revised March 8, 2017; Accepted March 31, 2017)

초록: 리그노술폰산(LSA)을 함유한 폴리피롤 복합체를 암모늄퍼설페이트 개시제를 사용하여 합성하였다. 이 때 포함시키는 리그노술폰산의 양은 달리 하였다. 합성된 폴리피롤 복합체에서 LSA가 폴리피롤 속에서 강한 화학 결합을 하고 있음을 UV와 IR 스펙트럼 방법과 표면성상 분석을 통해 확인하였다. 복합체의 온도 의존성 전도도 특성이 연구되었으며, 아울러 전도도 값을 통하여 전자 이동에 관한 활성화 에너지를 계산해보았다. 전기전도도는 LSA의 양이 증가할수록 증가하였는데, 이 결과는 LSA에 의한 전자 활성에 기인하는 것으로 여겨진다.

Abstract: Polypyrrole (PPy) composites containing lignosulfonic acid (LSA) were prepared via the polymerization of pyrrole monomer with different concentrations (wt%) of LSA sodium salt using ammonium persulfate as an oxidant. The strong interaction of LSA with PPy to form PPy-LSA composites was supported by spectral characterization and surface morphological studies. The electrical properties of the composite films were examined through temperature-dependent direct current conductivity measurements at 300-500 K to understand the conduction behavior of the composites. The activation energy for electron transport was also calculated based on the conductivity data. The conductivity of the films was increased by increasing LSA concentration (wt%) in the PPy-LSA composites. The result can be attributed to the increased mobility of the charge carriers by the increased concentration of LSA in the composites. The incorporation of LSA in PPy can cause the cost-effective transformation of the conductive polymer of PPy into a biodegradable polymer.

Keywords: lignosulfonic acid, electrical conductivity, polypyrrole, polymer composite.

Introduction

Conducting polymers, such as polypyrrole (PPy), have attracted considerable interest because of their diverse structures, special doping mechanism, excellent environmental stability, good solution processability, corrosion resistance, and high conductivity.[1,2] PPy has aroused increasing attention because of its practical applications based on its unparalleled architectural diversity and flexibility, excellent environmental stability, high conductivity, relatively low density, and ease of preparation.[3,4] Bulk quantities of PPy can be obtained in fine powder state prepared by the oxidative polymerization by using selected transition metal ions in water or other solvents.[5-9] The insolubility of conducting polymers in common solvents and their infusibility render them poorly processable either via a solution technique or melt-processing methods.[9,10] These material properties can be improved by forming either pyrrole copolymers or PPy composites with commercially available polymers or inorganic materials that offer good mechanical and optical properties, stability, and processability.[11,12] In general, PPy composites are synthesized through the *in situ* polymerization of pyrrole in the presence of organic or inorganic substances. Blending with soluble matrix polymers also improves the processability and mechanical properties of insoluble polymers.

In consideration of the great threat posed by synthetic poly-

†To whom correspondence should be addressed.
E-mail: chemhds@inje.ac.kr

mers to ecology, the use of renewable natural and thus biodegradable polymers to develop or improve existing materials or technologies is an important subject of research. However, research based on biodegradable polymer composites is limited compared with that based on nondegradable polymer composites because of the relatively poor availability and high price of biodegradable polymers.[13,14] The development of biodegradable polymer composites promotes the use of environment-friendly materials. The use of green materials provides alternative ways to solve the problems associated with nondegradable residues. Biodegradable polymers do not face the problem of exhaustion because they are prepared from renewable resources.

Lignin is a complex natural polymer that can be isolated from lignocellulosic materials. This aromatic network polymer has found applications in numerous industrial areas because of its versatile dispersing, binding, complexing, and emulsifying properties. The basic building blocks of lignin are variously substituted phenylpropane units, linked together via different chemical bonds, such as ether, alkyl, and aryl linkages.[15] Lignin-based polymers present twofold advantage. First, these polymers are abundantly available, given that tons of lignin is disposed as a waste product in the pulp and paper industries. Second, lignin is completely biodegradable, although the process takes time. Thus, lignin is a prospective biodegradable polymer. Sodium lignosulfonates (e.g., lignosulfonic acid (LSA) sodium salt) are used in the food industry as a defoaming agent for paper production and in adhesives for items that come in contact with food. These compounds have antimicrobial and preservative properties, and are used as an ingredient in animal feeds. Lignin is a macromolecular compound more chemically active than cellulose or other natural polymers because of the functional groups contained in its macromolecule. Thus, lignin is considered the main aromatic component of plant tissues. Lignin is globally regarded as a raw material featuring a high recovery potential, accessibility from renewable sources, low cost, and negligible pollution degree.[16,17] LSA contains sulfonate and hydroxyl groups resulting in a high reactivity under eco-friendly reaction conditions.[18] LSA is water soluble and contains sulfonated groups that possibly interact with pyrrole monomer during the polymerization of pyrrole to form PPy. PPy polymer composites expectedly contain LSA, which improves the physical and electrical properties of the composites.

In the present study, we prepared new types of PPy polymer composites containing different concentrations (wt%) of biodegradable and easily available materials, such as LSA. The prepared composites were characterized through Fourier-transform infrared spectroscopy (FTIR), UV-vis absorption spectroscopy (UV-vis), and X-ray diffraction analysis (XRD). The surface morphology of the resulting composites was examined via scanning electron microscopy (SEM) and transmission electron microscopy (TEM). The temperature-dependent direct current (DC) conductivity of the polymer composites in relation to the LSA concentration was also investigated for possible future applications.

Experimental

Materials. Analytical reagent-grade pyrrole, LSA sodium salt, and ammonium persulfate (APS) were purchased from Sigma-Aldrich, USA. *N*-methyl-2-pyrrolidinone (NMP) was obtained from Junsei Chemical Co., Japan.

Preparation of PPy and PPy-LSA Polymer Composites. In a typical procedure, 0.6 M pyrrole and LSA were mixed with 200 mL of distilled water and stirred for 30 min. This solution was slowly added with 0.12 M APS in distilled water and then continuously stirred at 400 rpm for 5 h while maintaining at room temperature. The reaction mixture was filtered under suction and then washed with distilled water and acetone. The product obtained was dried under vacuum for more than 24 h at room temperature. The LSA in the composites had varied target mass loadings of 20, 40, and 50 wt%. The composites with 20, 40, and 50 wt% of LSA in PPy will be abbreviated as PPy-LSA-1, PPy-LSA-2, and PPy-LSA-3, respectively. For the comparison, pure PPy was also synthesized without LSA.

A typical scheme for the formation of PPy-LSA composites is shown in Figure 1. In detail, LSA was initially added to a beaker containing 200 mL of distilled water, and the mixture was stirred until the complete dissolution of LSA. The monomer pyrrole was added slowly dropwise to the beaker containing LSA solution with continued stirring. After mixing pyrrole with the LSA-containing solution, the mixture changed into a slight dark solution, and a pyrrole-LSA complex formed while mixing. APS was added slowly to this reaction mixture through a dropwise addition, and the solution was allowed for approximately 4-5 h with continued stirring to form the PPy-LSA composites. Figure 1 schematically illustrates how the structure of LSA stabilizes the dispersed PPy. The fibrillar structure of LSA absorbs the pyrrole particles to form the pyrrole-LSA complex. The polymerization of pyrrole produces

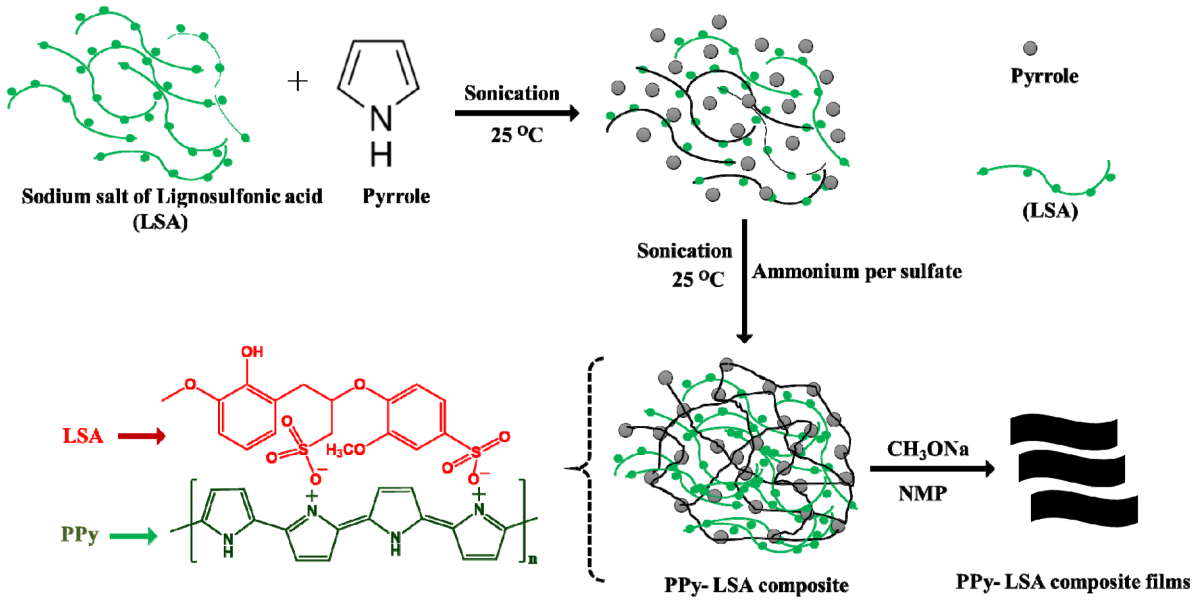

Figure 1. Overall scheme for the formation of PPy-LSA composite films.

PPy-LSA composites with chains of PPy entrapped within the LSA matrix. The characterization, preparation of thin films from the prepared PPy and PPy-LSA polymer composites, and measurement of DC conductivity were performed as previously described.[19,20]

Results and Discussion

Characterization of PPy and the PPy-LSA Polymer Composites. Figure 2 shows the FTIR spectra of LSA, PPy, PPy-LSA-1, PPy-LSA-2, and PPy-LSA-3, respectively. The FTIR spectrum of LSA reveals the peak at 3400 cm^{-1}, which corresponds to the -OH, N-H, and -SO_3H stretching vibrations. The bands around 790 and 690 cm^{-1} can be described as the out-of-plane vibrations of the substituted benzene rings in the structure of LSA. The absorption peaks at 1185 and 1050 cm^{-1} are attributed to the vibrations of sulfonic group, whereas the asymmetric C-H deformations of aromatic rings are indicated at 1465 cm^{-1}. The peaks at 805 and 914 cm^{-1} are attributed to C-H wagging.[21-23] The characteristic peaks at 1550 and 1465 cm^{-1} correspond to C=C stretching, whereas those at 1689 and 1315 cm^{-1} represent C=N and C-N bonds, respectively.[24] The occurrence of small peaks at 3515 cm^{-1} is assigned to N-H stretching vibrations. The peaks of PPy observed in the present work are well matching with the peaks reported in the previous studuies,[25] suggesting the formation of PPy. Some of the stretching vibrations of both LSA and PPy

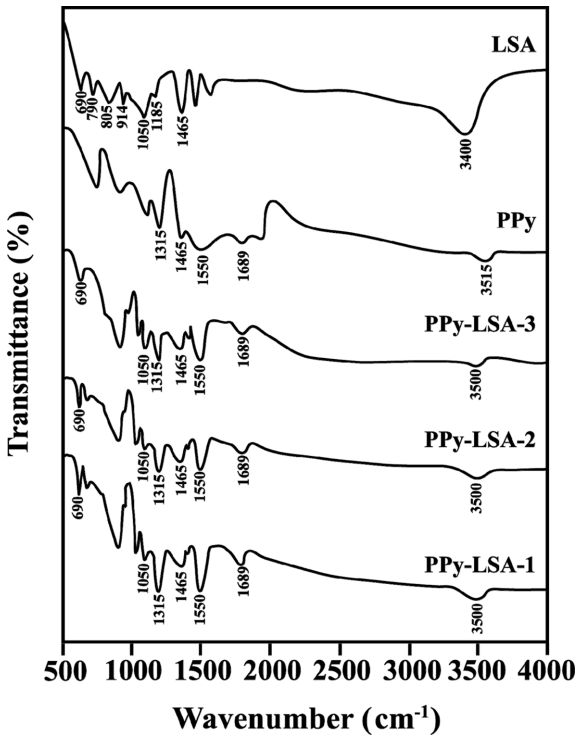

Figure 2. FTIR spectra of LSA, PPy, PPy-LSA-1, PPy-LSA-2, and PPy-LSA-3.

appear after the PPy-LSA composite formation of PPy-LSA-1, PPy-LSA-2, and PPy-LSA-3. These observations suggest the formation of PPy-LSA composites.

Figure 3 shows the UV-vis spectra of PPy and PPy-LSA

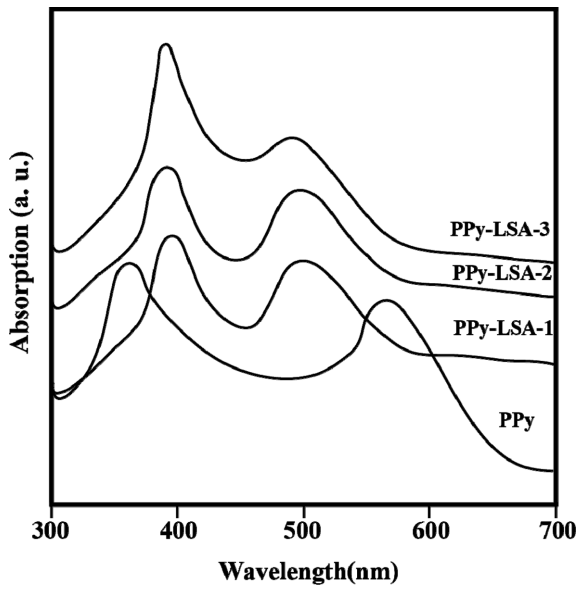

Figure 3. UV-vis spectra of PPy and the PPy-LSA polymer composites in NMP solution.

polymer composites. PPy and PPy-LSA in a 4 mg/mL solution with NMP as the solvent were subjected to UV-vis analysis. PPy shows two sharp peaks at 360 and 600 nm.[26] The peak at 360 nm corresponds to the absorption bands of π-π* transition, polaron, and bipolaron. The additional band at 600 nm shows the extension of conjugation in the polymer chain. The incorporation of LSA in the PPy matrix causes the shift of these peaks. The peak at 360 nm is red-shifted, whereas the peak at 600 nm is blue-shifted compared with the peaks in PPy. The change in peak positions suggests that a modification in the electronic structure and a relocation of polaron levels in PPy occur because of the incorporation of LSA. These UV-vis analysis results support the formation of the PPy-LSA composites.

Figures 4(a)-4(d) show the SEM images of (a) pure PPy, (b) PPy-LSA-1, (c) PPy-LSA-2, and (d) PPy-LSA-3, respectively. PPy shows an agglomerated spherical-like morphology. The approximate sizes of the spherical-like particles range from 20 to 25 nm. The SEM image of PPy-LSA-1 shows spherical-like structures of PPy and small granular particles. The small granular structures are caused by the presence of LSA in PPy. The concentration of small granular particles is increased in PPy-LSA-2. The concentration of small granular particles in PPy-LSA-3 increases with increasing LSA concentration (wt%). These small granular particles overlap with the spherical-like particles of PPy. The concentration of small granular particles also apparently increases with increasing LSA concentration.

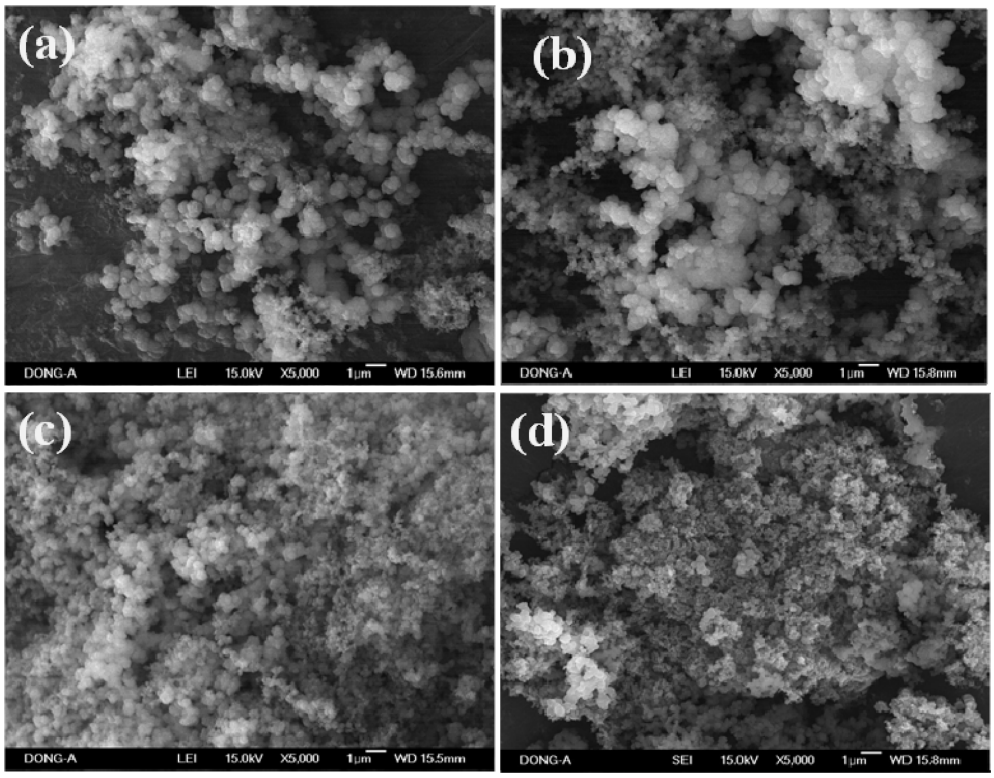

Figure 4. SEM images of (a) PPy; (b) PPy-LSA-1; (c) PPy-LSA-2; (d) PPy-LSA-3.

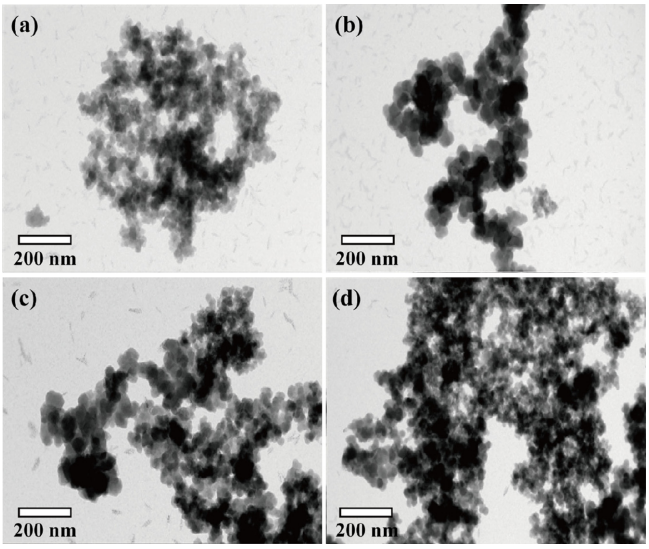

Figure 5. TEM images of (a) PPy; (b) PPy-LSA-1; (c) PPy-LSA-2; (d) PPy-LSA-3.

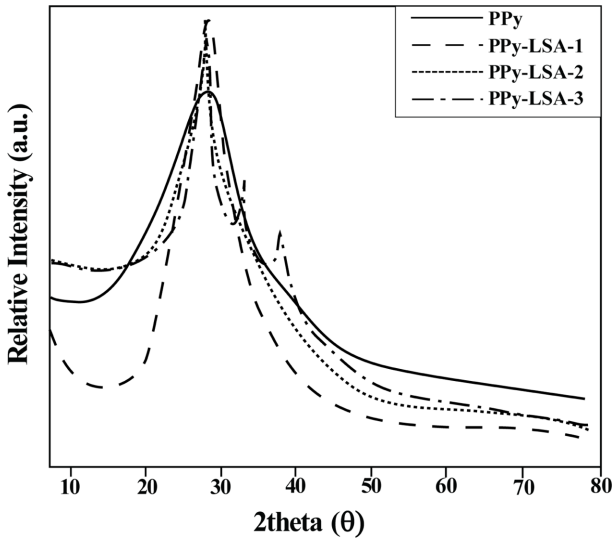

Figure 6. X-ray powder diffraction patterns of PPy and the PPy-LSA polymer composites.

Figures 5(a)-5(d) show the TEM images of (a) pure PPy, (b) PPy-LSA-1, (c) PPy-LSA-2, and (d) PPy-LSA-3. The TEM results of PPy and the PPy-LSA composites are similar to the SEM results. The TEM image of pure PPy shows small granular-like structures attached to one another to form a bulky structure. The TEM images of PPy-LSA-1 and PPy-LSA-2 show gray granular-like structures and black granular structures are interconnected with one another to form a bulky structure, respectively. The findings in Figure 4(d) are similar to those in Figure 5(d). That is, the concentration of small granular particles in PPy-LSA-3 increases with increasing LSA concentration. These small granular particles also overlap with the spherical-like particles of PPy.

Table 1 shows the atomic and weight percentages of C, S, N, and O obtained from the SEM-EDS data for PPy, PPy-LSA-1, PPy-LSA-2, and PPy-LSA-3, respectively. Table 1 shows a decrease in the percentage of C and an increase in those of S and O in the PPy-LSA composites. The decreased percentage of C in the PPy-LSA composites can be attributed to the increase in LSA concentration. The increase in the percentages of S and O may be caused by the partial oxidation of PPy with LSA chains during the formation of the PPy-LSA composites. Therefore, we can suggest the formation of the PPy-LSA polymer composites on the basis of the surface morphology studies and the EDS data for PPy, PPy-LSA-1, PPy-LSA-2, and PPy-LSA-3, respectively.

Figure 6 shows the X-ray diffraction patterns of PPy and the PPy-LSA polymer composites. The diffraction pattern of PPy shows a nearly broad peak between 2θ values of 20° and 30°; this peak is characteristic of PPy and indicates the amorphous nature of this polymer.[27,28] However, PPy-LSA-1 and PPy-LSA-2 indicate that the diffraction peak of 2θ at 20°-30° becomes increasingly sharp with increasing LSA concentration in PPy. The diffraction pattern of PPy-LSA-3 shows that the diffraction peak of 2θ at 20°-30° becomes sharp and that two other peaks appear at 32° and 37° as the LSA concentration is further increased. This finding indicates that the diffraction patterns of PPy-LSA-3 encompass a higher level of crystal-

Table 1. Atomic and Weight Percentage Data Obtained from EDS Spectra for PPy and PPy-LSA Polymer Composites

Element	Atomic %				wt%			
	C	S	O	N	C	S	O	N
PPy	85.35			7.66	79.78			19.78
PPy-LSA-1	78.42	2.13	13.03	5.15	70.56	5.62	19.82	3.5
PPy-LSA-2	76.15	2.43	17.07	2.56	68.90	5.80	23.01	2.22
PPy-LSA-3	73.36	3.37	19.27	1.85	65.76	6.50	25.55	1.95

linity than those of PPy-LSA-1 and PPy-LSA-2. Based from the diffraction patterns of the PPy-LSA composites, we can suggest that the incorporation of LSA is responsible for the increased crystallinity of PPy.

Temperature Dependent Conductivity of PPy and PPy-LSA Polymer Composites. The temperature-dependent DC conductivity of the PPy and PPy-LSA films was measured at 300-500 K. At first, the temperature-dependent resistance of PPy, PPy-LSA-1, PPy-LSA-2, and PPy-LSA-3 at 300-500 K was measured as shown in Figure 7. On the basis of the data in Figure 7, the temperature coefficient of resistivity (TCR) at 303-353, 353-403, and 403-453 K was calculated using the following eq. (1).[20,29]

$$\mathrm{TCR} = \left(\frac{1}{\rho(T_1)}\right)\left(\frac{\Delta\rho}{\Delta T}\right) \quad (1)$$

where, $\Delta\rho = \rho(T_1) - \rho(T_2)$ and $\Delta T = T_2 - T_1$. The TCR values of PPy, PPy-LSA-1, PPy-LSA-2, and PPy-LSA-3 are listed in Table 2. The TCR values of PPy at 303-353, 353-403, and 403-453 K were 7.35×10^{-4}, 0.0011, and 0.0012, respectively. The TCR values of PPy-LSA-1 in the preceding temperature ranges are 0.002, 0.0031, and 0.0035, respectively, whereas those of PPy-LSA-2 are 0.0032, 0.004, and 0.0046, respectively. Similarly, the TCR values of PPy-LSA-3 at 303-353, 353-403, and 403-453 K are 0.0014, 0.002, and 0.0025, respectively.

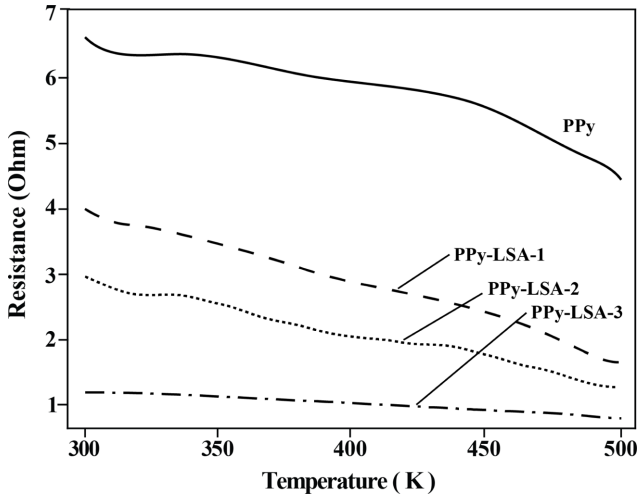

Figure 7. Temperature (K)-dependent resistance (Ohm) for the films of PPy, PPy-LSA-1, PPy-LSA-2, and PPy-LSA-3 at 300-500 K.

Table 2. Calculated Values of the Temperature Coefficient of Resistivity (TCR) for PPy and PPy-LSA Polymer Composites at Different Temperature Ranges

Temperature (K)	Temperature coefficient of resistivity (TCR)			
	PPy	PPy-LSA-1	PPy-LSA-2	PPy-LSA-3
303-353	7.35×10^{-4}	0.0020	0.0032	0.0014
353-403	0.0011	0.0031	0.0040	0.0020
403-453	0.0012	0.0035	0.0046	0.0025

Figure 8 represents the DC electrical conductivity as a function of temperature for PPy, PPy-LSA-1, PPy-LSA-2, and PPy-LSA-3. The room-temperature electrical conductivities of PPy, PPy-LSA-1, PPy-LSA-2, and PPy-LSA-3 are 0.15, 0.26, 0.325, and 0.82 S/cm, respectively. Similarly, the electrical conductivities at 503 K for PPy, PPy-LSA-1, PPy-LSA-2, and PPy-LSA-3 are 0.21, 0.62, 0.96, and 1.46 S/cm, respectively. The conductivities of the PPy-LSA composites increase with increasing temperature. The DC electrical conductivities of PPy and the PPy-LSA composites are very similar to a semiconducting behavior. This conductivity may be facilitated by the transport of electronic charges between PPy polymers as well as by the inclusion of LSA. The enhanced electrical conductivity is due to the formation of small granular particles of PPy, the facile flow of electron/charge carriers, and better network structure with the increase of LSA content. This mechanism is represented in the scheme shown in Figure 1 for the formation of PPy-LSA composites such as $PPy^{+}/\sim SO_3^{-}$ from LSA. By this proposed mechanism, the compatibility between PPy and ($\sim SO_3^{-}$) is much more enhanced.

Measurement of Activation Energy for PPy and the PPy-LSA Polymer Composites. Figure 8 shows a plot of

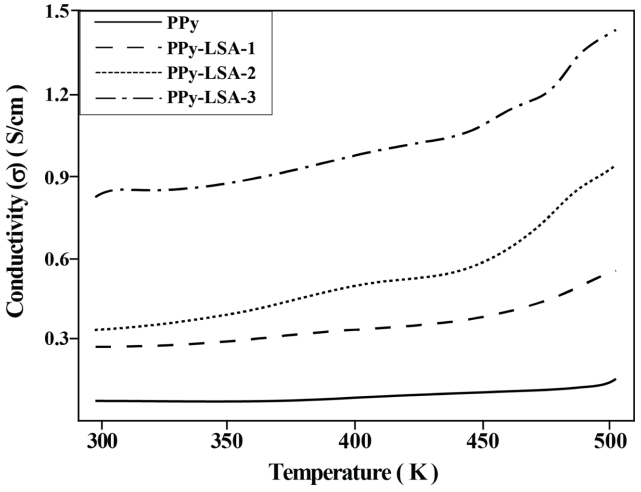

Figure 8. DC electrical conductivity (σ) *versus* temperature (K) for the films of PPy and the PPy-LSA polymer composites at 300-500 K.

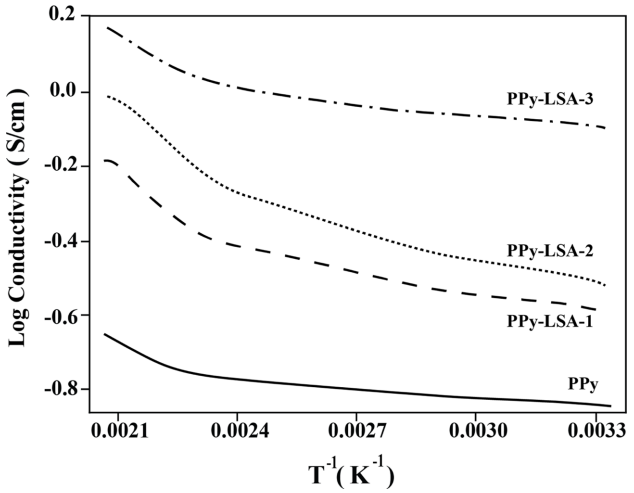

Figure 9. Plot of logarithmic conductivity *versus* inverse temperature for the films of PPy and the PPy-LSA polymer composites.

Table 3. Activation Energy (kJ/mol) for PPy and PPy-LSA Composites Obtained at Different Temperature Range

Polymer	298-403 K
PPy	2.21
PPy-LSA-1	1.98
PPy-LSA-2	1.79
PPy-LSA-3	1.65

conductivity *versus* temperature for PPy in, whereas the PPy-LSA composites apparently belong to two types of processes, namely, one in the range of 273-450 K (low temperature range) and the other in the range of 450-503 K (high temperature range). The values of activation energy (E_a) must be obtained for PPy, PPy-LSA-1, PPy-LSA-2, and PPy-LSA-3 to understand the conduction process. In general, σ can be expressed as

$$\sigma = \sigma_o \exp(-E_a/kT) \quad (2)$$

where, σ_o is the maximum conductivity and E_a is the activation energy.[29-32] The slope of the curve was obtained using the plot of logarithmic conductivity *versus* inverse temperature for PPy and the PPy-LSA polymer composites to obtain the E_a values. Figure 9 shows the plot of logarithmic conductivity *versus* inverse temperature for PPy, which shows a linear curve in the range of 0.0022 to 0.0033 K^{-1} with a negative slope. Table 3 shows the values of E_a in the range. The standard deviation of the activation energy is approximately ±5 kJ/mol. The enhancement in the temperature-dependent DC electrical conductivity of the PPy-LSA composites can be attributed to the flow of electron/charge carriers through the polymer chains of PPy, which is assisted by the presence of LSA. The temperature increase further assists the flow of charge carriers, thereby causing enhanced conductivity. As described in Figure 1, LSA forms a fibrillar structure encapsulating the pyrrole, and the polymerization of PPy forms a network-like structure. The formation of such a network-like structure may be responsible for the enhanced electrical conductivity.

Conclusions

New biodegradable PPy polymer composites containing sodium salt of LSA were prepared via the polymerization of pyrrole monomer with different concentrations (wt%) of LSA sodium salt using ammonium per sulfate as an oxidant. The incorporation of the LSA enhanced not only the electrical conductivity but also the surface morphology of the composites. The incorporation of LSA further increased the conductivity of the composites. The enhancement in the temperature-dependent DC electrical conductivity can be attributed to the flow of electrons/charge carriers through the polymer chains of PPy, which is assisted by the presence of LSA. Therefore, the incorporation of LSA in PPy can cause the cost-effective transformation of the conductive polymer of PPy into a biodegradable polymer. Also, the PPy-LSA composite host matrix has attractive potential applications in biosensors to study microorganisms. The new composites may also be benefit to the development of new applications for biomaterials in molecular electronics and other fields.

Acknowledgments: This research was supported by 2016 Inje University's Post Doc researcher supporting grant.

References

1. O. Mykhailiv, M. Imierska, M. Petelzyc, L. Echegoyen, and M. E. Plonska-Brzezinska, *Chemistry,* **21**, 5783 (2015).
2. J. Zhu, Y. Xu, J. Wang, J. Wang, Y. Bain, and X. Du, *Phys. Chem. Chem. Phys.*, **17**, 19885 (2015).
3. Q. Rong, H. Han, F. Feng, and Z. Ma, *Sci. Rep*., **5**, 11440 (2015).
4. H. Olsson, D. O. Carlsson, G. Nystrom, M. Sjodin, L. Nyholm, and M. Stromme, *J. Mater. Sci.,* **47**, 5317 (2012).
5. S. Machida, S. Miyata, and A. Techagumpuch, *Synth. Met.*, **31**, 311 (1989).
6. S. P. Armes, *Synth. Met.*, **20**, 365 (1987).
7. G. Xiong, P. K. Iyer, D. Moses, G. C. Bazan and A. J. Heegar, *Adv. Funct. Mater.*, **13**, 325 (2003).

8. T. H. Chao and J. J. March, *J. Polym. Sci.; Part A: Polym. Chem.*, **26**, 743 (1998).
9. Y. Wusheng, J. Li, Y. Li, J. Wu, and T. Gu, *J. Appl. Polym. Sci.*, **80**, 1368 (2001).
10. J. M. Machado, F. E. Karasz, and R. W. Lenz, *Polymer*, **29**, 1412 (1988).
11. M. A. D. Paoli, R. J. Waltman, A. F. Diaz, and J. Bargon, *J. Chem. Soc., Chem. Commun.*, **15**, 1015 (1984).
12. S. E. Lindsey and G. B. Street, *Synth. Met.*, **10**, 67 (1984).
13. G. Q. Chen and Q. Wu, *Biomaterials*, **26**, 6565 (2005).
14. T. Freier, *Adv. Polym. Sci.*, **203**, 1 (2016).
15. A. I. Pearl, *The Chemistry of Lignin*, Marcel Dekker Inc., New York, p 38 (1967).
16. A. M. Capraru, E. Ungureanu, and V. I. Popa, *EEMJ*, **7**, 525 (2008).
17. M. I. Totolin and G. Cazacu, *Adhesives, composite materials and other applications on the basis of lignin*, Pim Publishing House, Iaşi, p 195 (2010).
18. W. Chen, X. W. Peng, L. X. Zhong, Y. Li, and R. C. Sunm, *ACS Sustain. Chem. Eng.*, **3**, 1366 (2015).
19. C. Basavaraja, E. A. Jo, and D. S. Huh, *Polym. Compos.*, **32**, 79 (2011).
20. C. Basavaraja, W. J. Kim, D. G. Kim, and D. S. Huh, *Mater. Chem. Phys.*, **129**, 787 (2011).
21. G. Wang, B. Wang, J. Park, J. Yang, X. Shen, and J. Yao, *Carbon*, **47**, 68 (2009).
22. A. V. Murugan, T. Muraliganth, and A. Manthiram, *Chem. Mater.*, **21**, 5004 (2009).
23. H. J. Kharat, K. P. Kakade, P. A. Savale, K. Dutta, P. Ghosh, and M. D. Shirsat, *Polym. Adv. Tech.*, **18**, 397 (2007).
24. B. Tian and G. Zerbi, *J. Chem. Phys.,* **92**, 3886 (1990).
25. K. Arora, A. Chaubey, R. Singhal, R. P. Singh, M. K. Pandey, S. B. Samanta, B. D. Malhotra, and S. Chand, *Biosens. Bioelectron.*, **21**, 1777 (2006).
26. D. N. Huyen, N. T. Tung, T. D. Vinh, and N. D. Thien, *Sensors*, **12**, 7965 (2012).
27. A. Kassim, F. J. Davis, and G. R. Mitchell, *Synth. Met.*, **62**, 41 (1994).
28. C. Basavaraja, E. A. Jo, B. S Kim, D. G. Kim, and D. S. Huh, *Macromol. Res.*, **18**, 1037 (2010).
29. C. Basavaraja, R. Pierson, T. K. Vishnuvardhan, and D. S. Huh, *Eur. Polym. J.*, **44**, 1556 (2008).
30. C. Basavaraja, N. R. Kim, E. A. Jo, R. Pierson, D. S. Huh, and A. Venkataraman, *Bull. Korean Chem. Soc.*, **30**, 2701 (2009).
31. S. F. Yasin, A. M. Zihlif, and A. J. Ragosta, *J. Mater. Sci. Mater. Electron.*, **16**, 63 (2005).
32. X. S. Du, M. Xiao, and Y. Z. Meng, *Eur. Polym. J.*, **40**, 1489 (2004).